

# Adaptive Neural Network Control of Underactuated Surface Vessels with Guaranteed Transient Performance: Theory and Experimental Results

Lepeng Chen, Rongxin Cui, *Member, IEEE*, Chenguang Yang, *Senior Member, IEEE*, and Weisheng Yan

**Abstract**—In this paper, an adaptive trajectory tracking control algorithm for underactuated unmanned surface vessels (USVs) with guaranteed transient performance is proposed. To meet the realistic dynamical model of USVs, we consider that the mass and damping matrices are not diagonal and the input saturation problem. Neural Networks (NNs) are employed to approximate the unknown external disturbances and uncertain hydrodynamics of USVs. Moreover, both full state feedback control and output feedback control are presented, and the unmeasurable velocities of the output feedback controller are estimated via a high-gain observer. Unlike the conventional control methods, we employ the error transformation function to guarantee the transient tracking performance. Both simulation and experimental results are carried out to validate the superior performance via comparing with traditional potential integral (PI) control approaches.

**Index Terms**—Neural Network, underactuated surface vessel, guaranteed transient performance.

## I. INTRODUCTION

In the last decades, USV plays an important role in monitoring, exploration, surveillance and military applications. The accurate trajectory tracking control of USVs is a challenge because the precise model is unavailable and the external disturbances, such as ocean waves, currents, upward or downward streams and tides, can deteriorate the control performance.

Several control approaches have been proposed to relieve the effect of unknown disturbances and model uncertainties, such as sliding mode control [1]–[3], adaptive backstepping control [4]–[9], NN-based control [10]–[13], and neural learning control [14]–[16], model predictive control [17], [18], data-driven based control [19]–[21]. In [2], a novel sliding mode control strategy was presented for underactuated USV trajectory tracking by using a first-order and a second-order

sliding surface that based on surge and lateral tracking errors, respectively. In [6], an adaptive NN-based control for the realistic dynamical model of underactuated USVs that the mass and damping matrices are not diagonal was studied. In [22], to follow the sharp changing curvature, a path-following controller for USVs that based on disturbances observer was investigated. In [10], both full-state and output feedback adaptive neural control were proposed for USVs, and asymmetric barrier Lyapunov function was used to achieve output constraint. Based on the previous work, [14] presented an radial basis function (RBF) neural learning output feedback controller to steer an USV without velocity measurements. In [15], under the persistent excitation (PE) condition, a neural learning control of USVs was proposed with guaranteed performance. In [23], an online learning adaptive NN controller for small unmanned aerial rotorcraft was proposed to improve tracking performance via estimating the disturbances and eliminating their adverse effects, and experimental results verified the proposed controller. In [24], a fuzzy adaptive controller with simple form was proposed, and the global stability was proved for the system that under the unmodelled dynamics. In [19], a model-free iterative controller was presented to enhance the tuning performance via the designed criterion and measured closed loop data. The above-mentioned control schemes achieve good performance to address the problem of model uncertainties, external disturbances, unavailable velocity measurements, etc. Among these control techniques, the adaptive NN control is one of the most promising tools to improve the tracking performance of USVs that affected by the model uncertainties and disturbances.

However, some of the above-mentioned literatures only focused on the control of the fully actuated USV. In fact, most of USVs are underactuated with dynamic constraints, which have three degrees of freedom but only two control inputs are available for the control. Developing high-performance control algorithm for the underactuated USV under uncertainties and disturbances is an another challenging task in real applications. Tools to deal with the USV' underactuated control issue are focused on backstepping control and sliding mode control. In [25], a backstepping technique was proposed to control the underactuated USV under constant environmental disturbances. In [3], a sliding mode control was proposed to address the underactuated USV control problem, and experiments were carried out to verify the effectiveness.

Manuscript received October 17, 2018; revised February 01, 2019 and April 13, 2019; accepted April 18, 2019. This work was supported in part by the National Natural Science Foundation of China (NSFC) under grant U1813225, grant 61633002 and grant 61472325, and in part by the Science, Technology and Innovation Commission of Shenzhen Municipality under grant JCYJ20170817145216803, and in part by the Doctorate Foundation of Northwestern Polytechnical University under grant CX201904 (*Corresponding author: Rongxin Cui.*)

L. Chen, R. Cui and W. Yan are with the School of Marine Science and Technology, Northwestern Polytechnical University, Xi'an 710072, China. (email: r.cui@nwpu.edu.cn).

C. Yang is with the Bristol Robotics Laboratory, University of the West of England, Bristol BS16 1QY, U.K. (e-mail: cyang@ieee.org).

In real applications, the USV may be influenced by many obstacles such as submerged rocks in ocean. To ensure the safety of USVs, we need to guarantee the tracking errors remaining in a prescribed bounded region. Moreover, unconstrained maximum transient overshoot of the tracking errors can degrade the control performance, which may lead to a failing control. In addition, once the trajectory tracking errors violate the prescribed boundedness, in other words, the transformed errors become nonsense values, then USVs will stop working “automatically”, and it is a wonderful way to protect themselves. Therefore, guaranteeing transient performance is one of the most important issue and need to achieve in the control of USVs. In [26], a novel error transformation function was presented to restrict the maximum overshoot, convergence rate and steady-state error of strict feedback nonlinear systems with unknown nonlinearities. In [15], prescribed transient-performance-based neural learning controller was proposed to steer a fully actuated surface vessel with model uncertainties and disturbances. In [27], the tracking control problem with guaranteed transient performance was addressed for torpedo-like and unicycle-like underactuated underwater vehicles. In [28], a multi-layer NN robust controller was proposed for underactuated underwater vehicle with external disturbances and unmodeled dynamics, and the transient performance was achieved. In [29], a novel path following controller was proposed for USV with prescribed performance, and the nonlinear disturbance observers were designed to estimate the unknown disturbances.

The above papers are based on the assumption that mass and damping matrices of USVs are diagonal. However, in real model of USVs, this assumption is not tenable because the their shapes are not always semi-submerged sphere. In [30], the authors firstly relaxed the above assumption via introducing a coordinate transformation, which is crucial for controlling the underactuated USV. In [31], using the above coordinate transformation, a distributed containment control for USVs were proposed via backstepping technique. Noted that the designed controller for USVs in [3] is verified by experiment, and other controllers in [2], [4], [6], [12], [14], [15], [22], [25], [29]–[31] are verified by simulations.

In this paper, experiments are carried out to verify the effectiveness of the proposed controller. The USV that investigated in this paper only owns an inertial measurement unit (IMU) and a global positioning system (GPS), which are equipped to measure the attitude angle and position, respectively. In such a case, there is no direct sensor to measure USV’ velocity. To overcome the problem, output feedback controllers for USVs were proposed in [6], [32], [33].

Based on the above discussions, the difficulties of USVs control are focused on the effects of unknown external disturbances, input saturation, underactuated dynamic constrict, coupled and uncertain dynamic. Also, in real applications, guaranteeing the transient and steady-state tracking behavior can be an effective method to ensure the USV’ safety. It is meaningful to solve the above-mentioned issues simultaneously. Therefore, we design an adaptive NN control for an underactuated USV with guaranteed transient performance, and both the real dynamical model and the issue that without

velocity measurements are considered. Different from the control of fully actuated USVs with guaranteed transient performance in [5] and [10], we focus on the control law with underactuated manner. Also, compared with [4], we develop a NN-based controller that can guarantee the tracking errors’ transient and steady-state performance. Furthermore, unlike the results in [18] and [19], we develop the adaptive control without velocity measurements, which is much more matched the real applications. The difficulty of this work lies in the analysis of the control stability with rigorous mathematical theory when addressing both underactuated and transient performance guaranteed control problems. Moreover, performing lake experiments on the USV to verify the proposed controller is another difficulty.

The main contributions can be listed as follows.

- 1) A NN-based output feedback control is proposed for an underactuated USV that subject to the unknown external disturbances with transient tracking performance guaranteed. The transient behavior can be achieved via stabilizing the logarithm-based transformed errors, and the unmeasurable velocities are estimated by an observer.
- 2) An adaptive compensating approach and a state transformation are introduced to address the input saturation and dynamic coupled problems that existing in the realistic situation, respectively.
- 3) Rigorous theoretical analysis shows that all closed-loop signals are uniformly ultimately bounded (UUB) under the proposed control. Experimental studies are also carried out to validate the effectiveness of the proposed control.

The remainder of this paper is given as follows. Section II describes an underactuated USV dynamic and introduces some useful preliminaries. Section III proposes an adaptive NN controller for the underactuated USV with prescribed transient performance. Section IV and V show the simulational and experimental results, respectively.

## II. PRELIMINARIES AND PROBLEM FORMULATION

### A. Surface Vessel Dynamics

Motivated by [30], the nonlinear dynamics of the USV with unknown disturbances are provided as

$$\begin{aligned} \dot{\eta} &= J(\psi)\nu \\ M\dot{\nu} &= -C(\nu)\nu - D(\nu)\nu + d + \delta(\tau) \end{aligned} \quad (1)$$

where  $\eta = [x, y, \psi]^T$  denotes the position and yaw angle in the earth-fixed frame, respectively, which are shown in Fig. 1;  $\nu = [u, v, r]^T$  represents velocity states in surge  $u$ , sway  $v$ , and yaw  $r$  in the body-fixed frame;  $M = M^T$  is a non-diagonal inertia matrix,  $C$  and  $D$  are total Coriolis and Centripetal acceleration matrix, and damping matrix, respectively;  $d = [d_u, d_v, d_r]^T$  denotes the unknown disturbance; The saturated control vector  $\delta(\tau) = [\delta_1(\tau_1), 0, \delta_3(\tau_3)]^T = [\delta_1(\tau_u), 0, \delta_3(\tau_r)]^T$  is defined as

$$\delta_i(\tau_i) = \begin{cases} \tau_{i,\max}, & \text{if } \tau_i > \tau_{i,\max} \\ \tau_i, & \text{if } \tau_{i,\min} \leq \tau_i \leq \tau_{i,\max} \\ \tau_{i,\min}, & \text{if } \tau_i < \tau_{i,\min} \end{cases} \quad (2)$$

where  $i = 1, 3$ ,  $\tau = [\tau_1, 0, \tau_3]^\top = [\tau_u, 0, \tau_r]^\top$ ,  $\tau_u$  and  $\tau_r$  are USV's surge force and yaw moment, respectively; the bounds  $\tau_{i,\max}$  and  $\tau_{i,\min}$  are known. In addition, we define the dead-zero function as  $\chi = [\chi_u, 0, \chi_r]^\top = \tau - \delta(\tau)$ .

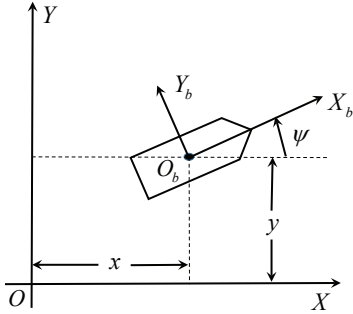


Fig. 1. Navigation and body frames of an USV.

In practical applications, it is difficult to obtain the accurate hydrodynamics coefficients of USV. Thus, we divide the above matrices into nominal part and bias part, i.e.,  $M = M^* + \Delta M$ ,

TABLE I  
NOMENCLATURE

| Symbol  | Description   |
|---|---|
| $\eta = [x, y, \psi]^\top \in \mathbb{R}^3$                                 | USV position and yaw angle in the earth-fixed frame                           |
| $\eta_d = [x_d, y_d, \psi_d]^\top \in \mathbb{R}^3$                         | Desired position and yaw angle in the earth-fixed frame                       |
| $\bar{\eta} = [\bar{x}, \bar{y}, \bar{\psi}]^\top \in \mathbb{R}^3$         | Transformed USV position and yaw  |
| $\bar{\eta}_d = [\bar{x}_d, \bar{y}_d, \bar{\psi}_d]^\top \in \mathbb{R}^3$ | Transformed Desired position and yaw angle                                    |
| $\nu = [u, v, r]^\top \in \mathbb{R}^3$                                     | USV velocities vector in the Body-fixed frame                                 |
| $\nu_v = [u_v, v_v, r_v]^\top \in \mathbb{R}^3$                             | Virtual USV velocities vector in the body-fixed frame                         |
| $\bar{\nu} = [u, \bar{v}, r]^\top \in \mathbb{R}^3$                         | Transformed USV velocities vector in the body-fixed frame                     |
| $[x_e, y_e, \psi_e]^\top \in \mathbb{R}^3$                                  | Positional tracking errors and yaw error                                      |
| $[e_x, e_y, e_\psi]^\top \in \mathbb{R}^3$                                  | Transformed tracking errors   |
| $[\rho_1, \rho_2, \rho_3]^\top \in \mathbb{R}^3$                            | Predefined bounded vector   |
| $\delta(\tau) \in \mathbb{R}^3$   | Saturated control inputs vector   |
| $\tau = [\tau_u, 0, \tau_r]^\top \in \mathbb{R}^3$                          | Control inputs vector   |
| $\chi = [\chi_u, 0, \chi_r]^\top = \tau - \delta(\tau)$                     | Dead-zero control inputs vector   |
| $J \in \mathbb{R}^{3 \times 3}$   | Jacobian matrix   |
| $M, M^*, \Delta M$  | Actual, nominal and bias part of inertia matrix                               |
| $C, C^*, \Delta C$  | Actual, nominal and bias part of Coriolis and Centripetal acceleration matrix |
| $D, D^*, \Delta D$  | Actual, nominal and bias part of damping matrix                               |
| $d \in \mathbb{R}^3$  | Unknown external disturbances   |
| $w \in \mathbb{R}^3$  | Time-varying disturbances in earth frame                                      |
| $d_{\text{sum}} \in \mathbb{R}^3$   | Sum of disturbance and uncertainties  |
| $s_1, s_2, s_3$   | Bias between virtual and estimated/actual velocities                          |

$C = C^* + \Delta C$  and  $D = D^* + \Delta D$ , where the bias part  $\Delta(\cdot)$  denotes the difference between the real value and the nominal value, and  $(\cdot)^*$  describes the nominal value that can be obtained from the tower tank experiment or the Computational Fluid Dynamics (CFD) analysis.

*Remark 1:* Unlike the conventional NN-based adaptive control for USV without any priori knowledge about the dynamics model parameters [19]–[21], we take full advantage of them to reduce the number of the NN node as well as computational complexity.

Now, the model of the USV can be rewritten as

$$M^* \dot{\nu} + C^*(\nu)\nu + D^*(\nu)\nu = \delta(\tau) + d_{\text{sum}} \quad (3)$$

where  $d_{\text{sum}} = -\Delta M \dot{\nu} - \Delta C(\nu)\nu + d$ , and

$$J(\psi) = \begin{bmatrix} \cos \psi & -\sin \psi & 0 \\ \sin \psi & \cos \psi & 0 \\ 0 & 0 & 1 \end{bmatrix}. \quad (4)$$

Since the real USVs are not semi-submerged sphere, their dynamic model are coupled, namely, their mass and damping matrices can not be assumed as diagonal. In such cases, it is difficult to design the control and analyze the stability. Therefore, motivated by [30], the state transforming method is employed to transform the mass matrix to a diagonal form, i.e.,  $\bar{v} = v + \varepsilon r$ ,  $\bar{x} = x + \varepsilon \cos \psi$ ,  $\bar{y} = y + \varepsilon \sin \psi$ , and  $\varepsilon = m_{23}^*/m_{22}^*$ . The model can be rewritten as

$$\begin{aligned} \dot{\bar{x}} &= u \cos \psi - \bar{v} \sin \psi, & \dot{u} &= \phi_u + \phi_{d1} + \delta_1(\tau_u)/m_{11}^* \\ \dot{\bar{y}} &= u \sin \psi + \bar{v} \cos \psi, & \dot{\bar{v}} &= \phi_v + \phi_{d2} \\ \dot{\psi} &= r, & \dot{r} &= \phi_r + \phi_{d3} + m_{22}^* \delta_3(\tau_r)/\Delta \end{aligned} \quad (5)$$

where  $\phi_u = \frac{m_{22}^*}{m_{11}^*} vr + \frac{m_{23}^*}{m_{11}^*} r^2 - \frac{d_{11}^*}{m_{11}^*} u$ ,  $\phi_v = -\frac{m_{11}^*}{m_{22}^*} ur - \frac{d_{22}^*}{m_{22}^*} v - \frac{d_{23}^*}{m_{22}^*} r$ ,  $\phi_r = \frac{1}{\Delta} \{(m_{11}^* m_{22}^* - m_{22}^{*2})uv + (m_{11}^* m_{23}^* - m_{22}^* m_{23}^*)ur - m_{22}^* (d_{33}^* r + d_{32}^* v) + m_{23}^* (d_{23}^* r + d_{22}^* v)\}$ ,  $\phi_{d1} = d_{\text{sum},u}/m_{11}^*$ ,  $\phi_{d2} = d_{\text{sum},v}/m_{22}^*$ ,  $\phi_{d3} = (-m_{23}^* d_{\text{sum},v} + m_{22}^* d_{\text{sum},r})/\Delta$ ,  $\Delta = m_{22}^* m_{33}^* - m_{23}^{*2}$ ; Furthermore,  $d_{ij}$ ,  $d_{ij}^*$ ,  $m_{ij}$  and  $m_{ij}^*$  represent the  $i$ th row and  $j$ th column of matrices  $D$ ,  $D^*$ ,  $M$  and  $M^*$ , respectively. We define that  $\bar{\eta} = [\bar{x}, \bar{y}, \bar{\psi}]^\top$  and  $\bar{\nu} = [u, \bar{v}, r]^\top$ .

## B. RBF Neural Networks

In this paper, to meet the real-time requirement in the applicable control system, we employ a traditional one layer RBF NNs to approximate the sum of uncertain hydrodynamics and unknown disturbances. The RBF NNs can estimate the real continuous function  $f$  as

$$f(Z) = \hat{f}(Z, W^*) + \varepsilon(Z), \quad \forall Z \in \Omega \quad (6)$$

where  $\varepsilon(Z)$  is a bounded approximation error satisfying  $|\varepsilon(Z)| \leq \varepsilon^*$ ;  $\hat{f}(Z, W^*) = W^{*\top} \Theta(Z)$ , the input vector  $Z \in \Omega$  in a compact set,  $W^*$  is the optimal NNs weights and it is defined as

$$W^* = \operatorname{argmin} \left[ \sup |f(Z) - \hat{f}(Z, \hat{W})| \right], Z \in \Omega \quad (7)$$

where  $\hat{W} = [\hat{W}_1, \dots, \hat{W}_N]^\top$  is the weight parameter vector, and  $N$  is NNs nodes number.  $\Theta(Z) = [\Theta_1(Z), \dots, \Theta_N(Z)]^\top$

is the nonlinear regressor vector of the inputs, which has the form as

$$\Theta_i(Z) = \exp \left[ -\frac{(Z - \xi_i)^\top (Z - \xi_i)}{\sigma_i^2} \right], i = 1, \dots, N \quad (8)$$

where  $\xi_i$  is the center of the  $i$ th basis function and  $\sigma_i$  represents the variance of  $i$ th basis function.

### C. Prescribed Transient Performance

We define the positional tracking errors and yaw error as  $x_e$ ,  $y_e$ ,  $\psi_e$ , respectively. To ensure the predefined transient performance, i.e., overshoot and convergence rate, we have

$$\begin{aligned} -\rho_1(t) < x_e(t) < \rho_1(t), \quad \forall t \geq 0 \\ -\rho_2(t) < y_e(t) < \rho_2(t), \quad \forall t \geq 0 \\ -\rho_3(t) < \psi_e(t) < \rho_3(t), \quad \forall t \geq 0 \end{aligned} \quad (9)$$

where  $\rho_i(t)$  is the predefined bounded function, which is described as

$$\rho_i(t) = (\rho_{i,0} - \rho_{i,\infty})e^{-\bar{\alpha}_i t} + \rho_{i,\infty} \quad i = 1, 2, 3 \quad (10)$$

where  $\rho_{i,0}$ ,  $\rho_{i,\infty}$  and  $\bar{\alpha}_i$  are positive constants. The overshoot and steady-state performance of tracking errors  $x_e$ ,  $y_e$  and  $\psi_e$  can be adjusted by the parameters of  $\rho_{i,0}$  and  $\rho_{i,\infty}$ . The  $\bar{\alpha}_i$  represents the predefined convergence rate.

To achieve the ‘‘constrained’’ tracking performance, the transformed errors are defined as

$$e_x = \Upsilon\left(\frac{x_e}{\rho_1}\right), \quad e_y = \Upsilon\left(\frac{y_e}{\rho_2}\right), \quad e_\psi = \Upsilon\left(\frac{\psi_e}{\rho_3}\right) \quad (11)$$

Meanwhile, the performance bounding functions  $\Upsilon$  in (11) can be chosen as

$$\Upsilon(z_i) = \ln \left( \frac{1 + z_i}{1 - z_i} \right), i = 1, 2, 3 \quad (12)$$

where  $z_1 = \frac{x_e}{\rho_1}$ ,  $z_2 = \frac{y_e}{\rho_2}$ ,  $z_3 = \frac{\psi_e}{\rho_3}$ .

*Remark 2:* [31] The function  $\Upsilon(z_i)$  owns two characters:  $\Upsilon(z_i)$  is a strictly increasing smooth function with bijective mappings  $\Upsilon(\cdot) : (-1, 1) \mapsto (-\infty, \infty)$ , and  $\Upsilon(0) = 0$ .

*Lemma 1:* [31] Consider the position and yaw errors  $x_e$ ,  $y_e$ ,  $\psi_e$ , and the transformed errors  $e_x$ ,  $e_y$ ,  $e_\psi$ . If the transformed errors are bounded, the prescribed transient performance of  $e_x$ ,  $e_y$  and  $e_\psi$  can be guaranteed.

### D. Problem Formulation

The objective of this paper is to develop a suitable control input  $\tau_u$  and  $\tau_r$  such that USV can track the desired trajectory  $\eta_d$  and the tracking errors  $x_e$ ,  $y_e$  and  $\psi_e$  can converge to a predefined bounds.

*Assumption 1:* The reference trajectory is defined as  $\dot{\eta}_d = J(\psi_d)\nu_d$ , then we have  $\dot{x}_d = u_d \cos \psi_d - v_d \sin \psi_d$ ,  $\dot{y}_d = u_d \sin \psi_d + v_d \cos \psi_d$ ,  $\dot{\psi}_d = r_d$ . where  $\eta_d = [x_d, y_d, \psi_d]^\top$ ,  $\nu_d = [u_d, v_d, r_d]^\top$ . We assume that  $u_d$ ,  $v_d$ ,  $\psi_d$  and their first derivatives are bounded. Furthermore, the external disturbance  $d$  is bounded.

*Lemma 2:* [34], [35] Since the saturation constraints of control inputs, we have that the velocities  $u$ ,  $v$ ,  $r$  are belonging to a compact set and bounded. Then, it is reasonable to assume

that the function  $\phi_u$ ,  $\phi_v$  and  $\phi_r$  are Lipschitz with respect to the velocity  $\nu$ .

*Proof:* According to hydrodynamic characteristic of USVs, the matrix  $C(\nu) + D(\nu)$  is positive. Therefore,  $M\dot{\nu} = -(C(\nu) + D(\nu))\nu + d + \delta(\tau)$  is a stable plant. Since  $d$  and  $\delta(\tau)$  are bounded, we can draw a conclusion that the velocities  $u$ ,  $v$ ,  $r$  are belonging to a compact set and bounded. Based on the facts that  $\phi_u$ ,  $\phi_v$  and  $\phi_r$  are continuous, we can infer that these functions are Lipschitz with respect to the velocity  $\nu$ . ■

Define the tracking error as

$$x_e = \bar{x} - \bar{x}_d, y_e = \bar{y} - \bar{y}_d, \psi_e = \psi - \psi_a \quad (13)$$

where  $\bar{x}_d = x_d + \varepsilon \cos \psi_d$ ,  $\bar{y}_d = y_d + \varepsilon \sin \psi_d$ . Motivated by [6],  $\psi_a$  is an angle that related to  $\psi_d$ ,  $x_e$  and  $y_e$ , which is defined as

$$\psi_a = \beta \tanh(D^2/a_1) + \psi_d ((1 - \tanh(D^2/a_1))) \quad (14)$$

where  $a_1$  is a positive constant, and  $\beta = \tan^{-1} \left( \frac{-y_e}{-x_e} \right)$ ,  $D = \sqrt{x_e^2 + y_e^2}$ .

## III. MAIN RESULTS

Based on the above-mentioned preliminaries and useful lemmas, we will design a full-state feedback and an output feedback controller for underactuated USVs in this section, respectively. NNs are employed to approximate the unknown external disturbances and uncertain dynamics.

### A. Adaptive Neural Network Control With Full-State Feedback

In this subsection, we will design a control law for USVs via using backstepping technique, which can guarantee the transient performance. Let us divide this control design phase into three steps: designing the appropriate virtual velocities, yielding the derivatives of transformed errors  $e_x$ ,  $e_y$  and  $e_\psi$ , deducing the derivatives of velocity errors  $s_1$ ,  $s_2$  and  $s_3$ .

Step 1: Design the appropriate virtual velocities to stabilize the transformed tracking errors. Motivated by [6], the errors between virtual and actual velocities can be defined as

$$\begin{aligned} s_1 &= u - u_v - \alpha_1 \tanh \beta_1, \\ s_2 &= v - v_v - \alpha_2 \tanh \beta_2, \\ s_3 &= r - r_v - \alpha_3 \tanh \beta_3 \end{aligned} \quad (15)$$

where  $\alpha_1$ ,  $\alpha_2$  and  $\alpha_3$  are positive constants,  $\nu_v = [u_v, v_v, r_v]^\top$  are virtual controls.

To stabilize the transformed tracking error,  $\nu_v$  can be designed as

$$\begin{aligned} u_v &= -l_1 e_x \cos \psi - l_1 e_y \sin \psi + \dot{\bar{x}}_d \cos \psi + \dot{\bar{y}}_d \sin \psi \\ v_v &= l_1 e_x \sin \psi - l_1 e_y \cos \psi - \dot{\bar{x}}_d \sin \psi + \dot{\bar{y}}_d \cos \psi \\ r_v &= -l_2 e_\psi + \dot{\psi}_d \end{aligned} \quad (16)$$

where  $l_1$  and  $l_2$  are positive constants. Furthermore,  $\beta_1$ ,  $\beta_2$  and  $\beta_3$  are given by

$$\begin{aligned} \dot{\beta}_1 &= \cosh^2 \beta_1 \{-\mu_u \beta_1 - \chi_u / m_{11}^*\} / \alpha_1 \\ \dot{\beta}_2 &= \cosh^2 \beta_2 \{\hat{W}_2^\top \Theta_2(Z) - l_3 s_1 + l_3 s_2 - l_3 s_3 + \phi_v\} / \alpha_2 \\ \dot{\beta}_3 &= \cosh^2 \beta_3 \{-\mu_r \beta_3 - m_{22}^* \chi_r / \Delta\} / \alpha_3 \end{aligned} \quad (17)$$

with positive constants  $l_3, \mu_u$  and  $\mu_r$ .

*Remark 3:* The virtual controls  $u_v, v_v$  and  $r_v$  are proposed to stabilize the transformed tracking errors  $e_x, e_y$  and  $e_\psi$  in kinematic level. Moreover,  $\beta_1$  and  $\beta_3$  are designed to compensate the effect of saturated inputs in (2), and  $\beta_2$  is proposed to deal with the problem of underactuation.

Step 2: Deduce the derivatives of transformed errors  $e_x, e_y$  and  $e_\psi$ . Differentiating both side of (13) along (5), we have

$$\begin{aligned}\dot{x}_e &= u \cos \psi - \bar{v} \sin \psi - \dot{\hat{x}}_d \\ \dot{y}_e &= u \sin \psi + \bar{v} \cos \psi - \dot{\hat{y}}_d \\ \dot{\psi}_e &= r - \dot{\psi}_a\end{aligned}\quad (18)$$

Using (12), we have  $u = s_1 + u_v + \alpha_1 \tanh \beta_1$ ,  $\bar{v} = s_2 + v_v + \alpha_2 \tanh \beta_2$ ,  $r = s_3 + r_v + \alpha_3 \tanh \beta_3$ . Substituting  $u, \bar{v}$  and  $r$  into (18), we have

$$\begin{aligned}\dot{x}_e &= (s_1 + u_v + \alpha_1 \tanh \beta_1) \cos \psi \\ &\quad - (s_2 + v_v + \alpha_2 \tanh \beta_2) \sin \psi - \dot{\hat{x}}_d \\ \dot{y}_e &= (s_1 + u_v + \alpha_1 \tanh \beta_1) \sin \psi \\ &\quad + (s_2 + v_v + \alpha_2 \tanh \beta_2) \cos \psi - \dot{\hat{y}}_d \\ \dot{\psi}_e &= (s_3 + r_v + \alpha_3 \tanh \beta_3) - \dot{\psi}_a\end{aligned}\quad (19)$$

Differentiating both side of (11), we have

$$\dot{e}_x = \frac{\rho_1 \dot{x}_e - x_e \dot{\rho}_1}{(1 - z_1^2) \rho_1^2}, \quad \dot{e}_y = \frac{\rho_2 \dot{y}_e - y_e \dot{\rho}_2}{(1 - z_2^2) \rho_2^2}, \quad \dot{e}_\psi = \frac{\rho_3 \dot{\psi}_e - \psi_e \dot{\rho}_3}{(1 - z_3^2) \rho_3^2}\quad (20)$$

Substituting (19) into (20), we have

$$\begin{aligned}\dot{e}_x &= \frac{-2l_1 e_x + 2s_1 \cos \psi - 2s_2 \sin \psi + \varphi_1}{\varrho_1} \\ \dot{e}_y &= \frac{-2l_1 e_y + 2s_1 \sin \psi + 2s_2 \cos \psi + \varphi_2}{\varrho_2} \\ \dot{e}_\psi &= \frac{-2l_2 e_\psi + 2s_3 + \varphi_3}{\varrho_3}\end{aligned}\quad (21)$$

where  $\varrho_i = (1 - z_i^2) \rho_i$ ,  $i = 1, 2, 3$ ,  $\varphi_1 = 2\alpha_1 \tanh \beta_1 \cos \psi - 2\alpha_1 \tanh \beta_1 \sin \psi + 2\dot{\rho}_1 z_1$ ,  $\varphi_2 = 2\alpha_2 \tanh \beta_2 \sin \psi + 2\alpha_2 \tanh \beta_2 \cos \psi - 2\dot{\rho}_2 z_2$ ,  $\varphi_3 = 2\alpha_3 \tanh \beta_3 - 2\dot{\psi}_a + 2\dot{\psi}_d - 2\dot{\rho}_3 z_3$ .

*Remark 4:* From the definition of  $\varphi_i, i = 1, 2, 3$ , we have: (i)  $|\tanh(\bullet)| \leq 1$ ,  $|\sin(\bullet)| \leq 1$ ,  $|\cos(\bullet)| \leq 1$ ; (ii) According to the Assumption 1, both terms of  $\dot{\hat{x}}_d, \dot{\hat{y}}_d$  and  $\dot{\psi}_a$  are bounded; (iii) From (12) and (10), we have  $|\Upsilon^{-1}(\cdot)| \leq 1$ ,  $|\dot{\rho}_i| \leq \alpha_i(\rho_{i,0} - \rho_{i,\infty})$ ,  $i = 1, 2, 3$ , respectively. We can draw a conclusion that there exist positive constants  $\bar{\varphi}_1, \bar{\varphi}_2$  and  $\bar{\varphi}_3$  satisfying  $\varphi_1 \leq \bar{\varphi}_1$ ,  $\varphi_2 \leq \bar{\varphi}_2$  and  $\varphi_3 \leq \bar{\varphi}_3$ .

Step 3: Deduce the derivatives of velocity errors  $s_1, s_2, s_3$  and the controls  $\tau_u, \tau_r$ . Differentiating both sides of  $s_1, s_2, s_3$  in (15) along (17), we have

$$\begin{aligned}\dot{s}_1 &= \dot{u} - \dot{u}_v + \mu_u \beta_1 + \chi_u / m_{11}^* \\ \dot{s}_2 &= \dot{\bar{v}} - \dot{v}_v - \hat{W}_2^\top \Theta_2(Z) + l_3 s_1 - l_3 s_2 + l_3 s_3 - \dot{\phi}_v \\ \dot{s}_3 &= \dot{r} - \dot{r}_v + \mu_r \beta_3 + m_{22}^* \tau_r / \Delta\end{aligned}\quad (22)$$

Because of the facts that  $\tau_u = \delta_1(\tau_u) + \chi_u$  and  $\tau_r = \delta_3(\tau_r) + \chi_r$ , and substituting (5) into (22), we have

$$\begin{aligned}\dot{s}_1 &= \phi_u + \phi_{d1} - \dot{u}_v + \mu_u \beta_1 + \tau_u / m_{11}^* \\ \dot{s}_2 &= \phi_{d2} - \dot{v}_v - \hat{W}_2^\top \Theta_2(Z) + l_3 s_1 - l_3 s_2 + l_3 s_3 \\ \dot{s}_3 &= \phi_r + \phi_{d3} - \dot{r}_v + \mu_r \beta_3 + m_{22}^* \tau_r / \Delta\end{aligned}\quad (23)$$

where  $Z = [u, v, r, u_v, v_v, r_v, e_x, e_y, e_\psi]^\top$  is the input of the NNs.

Then, the control and adaptive laws are designed as

$$\begin{aligned}\tau_u &= m_{11}^* \left( -l_3 s_1 - l_3 s_2 - \hat{W}_1^\top \Theta_1(Z) - \phi_u - \mu_u \beta_1 \right) \\ \tau_r &= \Delta \left( -l_3 s_2 - l_3 s_3 - \hat{W}_3^\top \Theta_3(Z) - \phi_r - \mu_r \beta_3 \right) / m_{22}^* \\ \dot{\hat{W}}_i &= \Gamma_i \left( \Theta_i(Z) s_i - \kappa_i \hat{W}_i \right), \quad i = 1, 2, 3\end{aligned}\quad (24)$$

where  $\kappa_i > 0$ .

Substituting (24) into (23), we have

$$\begin{aligned}\dot{s}_1 &= \phi_{d1} - \dot{u}_v - l_3 s_1 - l_3 s_2 - \hat{W}_1^\top \Theta_1(Z) \\ \dot{s}_2 &= \phi_{d2} - \dot{v}_v - \hat{W}_2^\top \Theta_2(Z) + l_3 s_1 - l_3 s_2 + l_3 s_3 \\ \dot{s}_3 &= \phi_{d3} - \dot{r}_v - l_3 s_2 - l_3 s_3 - \hat{W}_3^\top \Theta_3(Z)\end{aligned}\quad (25)$$

Define that  $\tilde{W}_1^* \Theta_1(Z) + \epsilon_1 = \phi_{d1} - \dot{u}_v$ ,  $\tilde{W}_2^* \Theta_2(Z) + \epsilon_2 = \phi_{d2} - \dot{v}_v$  and  $\tilde{W}_3^* \Theta_3(Z) + \epsilon_3 = \phi_{d3} - \dot{r}_v$ , we have

$$\begin{aligned}\dot{s}_1 &= -l_3 s_1 - l_3 s_2 - \tilde{W}_1^\top \Theta_1(Z) + \epsilon_1 \\ \dot{s}_2 &= l_3 s_1 - l_3 s_2 + l_3 s_3 - \tilde{W}_2^\top \Theta_2(Z) + \epsilon_2 \\ \dot{s}_3 &= -l_3 s_2 - l_3 s_3 - \tilde{W}_3^\top \Theta_3(Z) + \epsilon_3\end{aligned}\quad (26)$$

where  $\tilde{W}_i = \hat{W}_i - W_i^*$ ,  $i = 1, 2, 3$ .

*Remark 5:* To further illustrate the proposed controller, we draw a diagram in Fig. 2. The control scheme can be divided into kinematic and dynamic levels. In the kinematic level, we construct the virtual velocities to stabilize the transformational tracking errors. The goal of dynamic level is to ensure the virtual velocities can be tracked in the presence uncertainties via proposed control input  $\tau_u$  and  $\tau_r$ .

Since the objectives of this controller are to ensure  $e_x, e_y, e_\psi, s_i, \tilde{W}_i, i = 1, 2, 3$  converge to the small neighborhood of zero, then the Lyapunov function candidate can be defined as

$$V = V_1 + V_2 + V_3\quad (27)$$

where  $V_1 = \frac{1}{2} \varrho_1 e_x^2 + \varrho_2 e_y^2 + \varrho_3 e_\psi^2$ ,  $V_2 = \sum_{i=1}^3 s_i^2$  and  $V_3 = \sum_{i=1}^3 \tilde{W}_i^\top \Gamma_i^{-1} \tilde{W}_i$ .

*Theorem 1:* Consider the USV dynamics in (1) and the transformed dynamics in (5), together with the error transformed function in (11), the virtual controller in (16), the full-state feedback control and adaptive law in (24), and give the initial tracking error conditions that satisfying  $|e_x(0)| < \rho_{1,0}$ ,  $|e_y(0)| < \rho_{2,0}$ ,  $|e_\psi(0)| < \rho_{3,0}$ , the proposed full-state feedback controller can guarantee that: (i) the tracking errors are bounded by the prescribed function  $\rho_i$  and converge to a small neighborhood of zero; (ii) the signals in the closed loop system are UUB.

*Remark 6:* In practice, there are two methods to ensure the initial tracking errors in the bounds. Suitable path planning

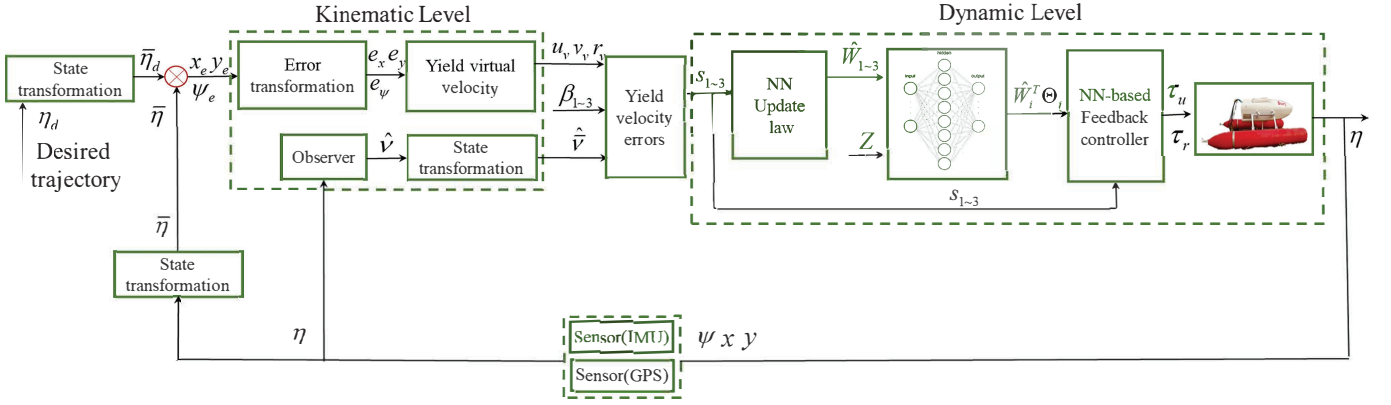


Fig. 2. Diagram of the proposed control system

algorithms can be utilized to yield an appropriate trajectory, which is in the neighborhood of the USV at the initial moment. By this method, we can guarantee the initial tracking errors in the predefined bounds. Also, appropriate choosing of the parameters  $\rho_{1,0}$ ,  $\rho_{2,0}$  and  $\rho_{3,0}$  is another method to keep the initial tracking error in the bounds.

*Proof:* Taking the derivative of  $V_1$ , and combing with (21), we have

$$\begin{aligned} \dot{V}_1 &= \varrho_1 e_x \dot{e}_x + \varrho_2 e_y \dot{e}_y + \varrho_3 e_\psi \dot{e}_\psi \\ &= -2l_1 e_x^2 - 2l_1 e_y^2 - 2l_2 e_\psi^2 + 2e_x(s_1 \cos \psi - s_2 \sin \psi) \\ &\quad + 2e_y(s_1 \sin \psi + s_2 \cos \psi) + 2e_\psi s_3 + e_x \varphi_1 \\ &\quad + e_y \varphi_2 + e_\psi \varphi_3 + \dot{\rho}_1 e_x^2 / 2 + \dot{\rho}_2 e_y^2 / 2 + \dot{\rho}_3 e_\psi^2 / 2 \\ &\leq -2l_1 e_x^2 - 2l_1 e_y^2 - 2l_2 e_\psi^2 + 2|e_x s_1| + 2|e_x s_2| \\ &\quad + 2|e_y s_1| + |e_y s_2| + 2|e_\psi s_3| + |e_x \varphi_1| + |e_y \varphi_2| \\ &\quad + |e_\psi \varphi_3| + \bar{\varrho}_1 e_x^2 / 2 + \bar{\varrho}_2 e_y^2 / 2 + \bar{\varrho}_3 e_\psi^2 / 2 \end{aligned} \quad (28)$$

Using the Young's inequality, (28) can be rewritten as

$$\begin{aligned} \dot{V}_1 &\leq -(2l_1 - 5/2 - \frac{\dot{\varrho}_1}{2})e_x^2 - (2l_1 - 5/2 - \frac{\dot{\varrho}_2}{2})e_y^2 \\ &\quad - (2l_2 - 3/2 - \frac{\dot{\varrho}_3}{2})e_\psi^2 + 2 \sum_{i=1}^3 s_i^2 + \frac{1}{2} \sum_{i=1}^3 \bar{\varphi}_i^2 \end{aligned} \quad (29)$$

Applying (26),  $\dot{V}_2$  can be written as

$$\begin{aligned} \dot{V}_2 &= s_1(-l_3 s_1 - l_3 s_2 - \tilde{W}_1^\top \Theta_1(Z) + \epsilon_1) \\ &\quad + s_2(l_3 s_1 - l_3 s_2 + l_3 s_3 - \tilde{W}_2^\top \Theta_2(Z) + \epsilon_2) \\ &\quad + s_3(-l_3 s_2 - l_3 s_3 - \tilde{W}_3^\top \Theta_3(Z) + \epsilon_3) \\ &= -l_3 \sum_{i=1}^3 s_i^2 - \sum_{i=1}^3 (s_i \tilde{W}_i^\top \Theta_i(Z) - s_i \epsilon_i) \end{aligned} \quad (30)$$

There is an positive constant satisfying that  $\epsilon_i \leq \epsilon_i^*$ . Since  $s_i \epsilon_i \leq (s_i^2 + \epsilon_i) / 2$ , we have

$$\dot{V}_2 \leq -\left(l_3 - \frac{1}{2}\right) \sum_{i=1}^3 s_i^2 - \sum_{i=1}^3 \left(s_i \tilde{W}_i^\top \Theta_i(Z) - \frac{\epsilon_i^{*2}}{2}\right) \quad (31)$$

Using the adaptive law in (24), the derivatives of  $V_3$  can be written as

$$\dot{V}_3 = \sum_{i=1}^3 \left( \hat{W}_i^\top \Theta_i(Z) s_i - \kappa_i \tilde{W}_i \right) \quad (32)$$

Applying the properties of RBFNN, we have

$$-\kappa_i \tilde{W}_i^\top \tilde{W}_i \leq \frac{\kappa_i}{2} \left( \|W_i^*\|^2 - \|\tilde{W}_i\|^2 \right) \quad (33)$$

Substituting (33) into (32), we have

$$\dot{V}_3 = \sum_{i=1}^3 \left( \hat{W}_i^\top \Theta_i(Z) s_i + \frac{\kappa_i}{2} \|W_i^*\|^2 - \frac{\kappa_i}{2} \|\tilde{W}_i\|^2 \right) \quad (34)$$

Since  $\varrho_i \leq \rho_{i,0}$ ,  $\dot{\varrho}_i \leq \bar{\varrho}_i$ , and combing (29), (31), (34),  $\dot{V}$  can be written as

$$\begin{aligned} \dot{V} &\leq -(2l_1 - 5/2 - \bar{\varrho}_1/2)e_x^2 - (2l_1 - 5/2 - \bar{\varrho}_2/2)e_y^2 \\ &\quad - (2l_2 - 3/2 - \bar{\varrho}_3/2)e_\psi^2 - (l_3 - 5/2)s_1^2 - (l_3 - 5/2)s_2^2 \\ &\quad - (l_3 - 3/2)s_3^2 - \sum_{i=1}^3 \frac{\kappa_i}{2} \|\tilde{W}_i\|^2 + C \\ &\leq -\mu V + C \end{aligned} \quad (35)$$

where

$$\begin{aligned} \mu &= \min \left( \frac{2l_1 - 5/2 - \bar{\varrho}_1/2}{\rho_{1,0}}, \frac{2l_1 - 5/2 - \bar{\varrho}_2/2}{\rho_{2,0}}, \right. \\ &\quad \left. \frac{2l_2 - 3/2 - \bar{\varrho}_3/2}{\rho_{3,0}}, l_3 - 5/2, \min \left( \frac{\kappa_i}{\lambda_{\max}(\Gamma_i^{-1})} \right) \right) \\ C &= \frac{1}{2} \sum_{i=1}^3 (\kappa_i \|W_i^*\|^2 + \epsilon_i^{*2} + \bar{\varphi}_i^2) \end{aligned}$$

where  $\lambda_{\max}(\bullet)$  denotes the maximum eigenvalues of  $\bullet$ . To guarantee the positive of  $\mu$ , the control gains  $l_1, l_2$  and  $l_3$  should be chosen to satisfy the following conditions:

$$\begin{aligned} l_1 &\geq \max(\bar{\varrho}_1/4 + 5/4, \bar{\varrho}_2/4 + 5/4) \\ l_2 &\geq \bar{\varrho}_3/4 + 3/4, \quad l_3 \geq 5/2 \end{aligned} \quad (36)$$

Multiplying on both sides by  $e^{\mu t}$ , we have

$$V(t) \leq (V(0) - C/\mu) \exp(-\mu t) + C/\mu, \quad \forall t > 0 \quad (37)$$

From the above inequality, and applying the definition of  $V$  in (27), we can draw a conclusion that the transformed errors  $e_x, e_y, e_\psi, s_i$  as well as the NN weight estimation errors  $\tilde{W}_i$  are bounded. In terms of the boundedness of transformed errors and according to Lemma 1, we can conclude that tracking error constraints  $x_e, y_e, \psi_e$  are never violated, i.e.,  $|x_e(t)| < \rho_1(t)$ ,  $|y_e(t)| < \rho_2(t)$ ,  $|\psi_e(t)| < \rho_3(t)$ . This completes the proof.  $\blacksquare$

### B. Adaptive Neural Network Control With Output Feedback

The state-feedback control is based on the condition that the velocities  $u, v, r$  can be measured via sensors, i.e., Inertial Navigation System (INS) or Doppler Velocity Log (DVL), etc. However, these sensors are too expensive. To deal with the problem, we employ a high-gain observer to estimate the unmeasurable velocities. In this subsection, we will propose an output feedback control for the underactuated USV.

Consider the following system:

$$\begin{aligned} \gamma \dot{b}_1 &= b_2 \\ \gamma \dot{b}_2 &= -\lambda_1 b_2 - b_1 + \eta \end{aligned} \quad (38)$$

where  $\gamma$  is a small positive constant,  $b_1, b_2 \in \mathbb{R}^3$  are states.

Using the result of [8, Lemma 3],  $\exists t > t^*$ , the estimate error  $\frac{b_2}{\gamma} - \eta$  is UUB. Therefore, we use  $b_2/\gamma$  to estimate  $\eta$ .

According to the definition of  $J(\psi)$  in (4), we have  $J^\top = J^{-1}$ . Thus, the unmeasurable velocities  $\nu$  and  $s = [s_1, s_2, s_3]^\top$  can be estimated as

$$\hat{\nu} = J^\top b_2/\gamma, \quad \hat{s} = \hat{\nu} - \nu_v, \quad \tilde{s} = \hat{s} - s = J^\top \xi_2 \quad (39)$$

Using the full-state feedback control law in (24), we can rewrite the output feedback controller as

$$\begin{aligned} \tau_u &= m_{11}^* \left( -l_3 \hat{s}_1 - l_3 \hat{s}_2 - \hat{W}_1^\top \Theta_1(\hat{Z}) - \hat{\phi}_u - \mu_u \beta_1 \right) \\ \tau_r &= \Delta \left( -l_3 \hat{s}_2 - l_3 \hat{s}_3 - \hat{W}_3^\top \Theta_3(\hat{Z}) - \hat{\phi}_r - \mu_r \beta_3 \right) / m_{22}^* \\ \dot{\hat{W}}_i &= \Gamma_i \left( \Theta_i(\hat{Z}) s_i - \kappa_i \hat{W}_i \right), \quad i = 1, 2, 3 \end{aligned} \quad (40)$$

where  $\hat{Z} = [\hat{u}, \hat{v}, \hat{r}, u_v, v_v, r_v, e_x, e_y, e_\psi]^\top$ ,  $\kappa_i > 0$  for all  $i = 1, 2, 3$ .

**Theorem 2:** Consider the USV dynamics in (1) and the transformed dynamics in (5), together with the error transformed function in (11), the virtual controller in (16), the high-gain observer in (38), (39), the output feedback control and adaptive law in (40), and give the initial tracking error conditions satisfy that  $|e_x(0)| < \rho_{1,0}$ ,  $|e_y(0)| < \rho_{2,0}$ ,  $|e_\psi(0)| < \rho_{3,0}$ , then the proposed full-state feedback controller can guarantee that: (i) the tracking errors are bounded by the prescribed function  $\rho_i$  and converge to a small neighborhood of zero; (ii) the signals in the closed loop system are UUB.

*Proof:* The Lyapunov function  $V$  is defined in (27). Substituting (40) into (23), we have

$$\begin{aligned} \dot{s}_1 &= -l_3 \hat{s}_1 - l_3 \hat{s}_2 - \tilde{\phi}_u - \hat{W}_1^\top \Theta_1(\hat{Z}) + W_1^{*\top} \Theta_1(Z) + \epsilon_1 \\ \dot{s}_2 &= l_3 \hat{s}_1 - l_3 \hat{s}_2 + l_3 \hat{s}_3 - \tilde{\phi}_v - \hat{W}_2^\top \Theta_2(\hat{Z}) + W_2^{*\top} \Theta_2(Z) + \epsilon_2 \\ \dot{s}_3 &= -l_3 \hat{s}_2 - l_3 \hat{s}_3 - \tilde{\phi}_r - \hat{W}_3^\top \Theta_3(\hat{Z}) + W_3^{*\top} \Theta_3(Z) + \epsilon_3 \end{aligned} \quad (41)$$

where  $\tilde{\phi}_u = \hat{\phi}_u - \phi_u$ ,  $\tilde{\phi}_v = \hat{\phi}_v - \phi_v$  and  $\tilde{\phi}_r = \hat{\phi}_r - \phi_r$ .

Applying (40), (26) and (21), the  $\dot{V}$  can be given as

$$\begin{aligned} \dot{V} &= \varrho_1 e_x \dot{e}_x + \varrho_2 e_y \dot{e}_y + \varrho_3 e_\psi \dot{e}_\psi + \sum_{i=1}^3 s_i \dot{s}_i + \sum_{i=1}^3 \tilde{W}_i \Gamma_i^{-1} \dot{\tilde{W}}_i \\ &= -2l_1 e_x^2 - 2l_1 e_y^2 - 2l_2 e_\psi^2 - l_3 \sum_{i=1}^3 s_i^2 + 2e_x(s_1 - s_2) \\ &\quad + 2e_y(s_1 + s_2) + 2e_\psi s_3 + \sum_{i=1}^3 s_i g_i(\bullet) + e_x \varphi_1 \\ &\quad + e_y \varphi_2 + e_\psi \varphi_3 + \dot{\varrho}_1 e_x^2 + \dot{\varrho}_2 e_y^2 + \dot{\varrho}_3 e_\psi^2 \\ &\quad + \sum_{i=1}^3 \left( -s_i \hat{W}_i^\top \Theta_i(\hat{Z}) + s_i W_i^{*\top} \Theta_i(Z) + s_i \epsilon_i \right) \\ &\quad + \sum_{i=1}^3 \left( \tilde{W}_i^\top \Theta_i(\hat{Z}) s_i - \kappa_i \tilde{W}_i^\top \hat{W}_i \right) \end{aligned} \quad (42)$$

where  $g_1(\bullet) = -l_3 \tilde{s}_1 - l_3 \tilde{s}_2 - \tilde{\phi}_u$ ,  $g_2(\bullet) = l_3 \tilde{s}_1 - l_3 \tilde{s}_2 + l_3 \tilde{s}_3 - \tilde{\phi}_v$ ,  $g_3(\bullet) = -l_3 \tilde{s}_2 - l_3 \tilde{s}_3 - \tilde{\phi}_r$ . Using Lemma 2, under Assumption 1, we can conclude that there exist positive constants  $p_i, i = 1, \dots, 4$  satisfying  $\sum_{i=1}^3 s_i g_i(\bullet) \leq \sum_{i=1}^3 (p_i s_i^2) + p_4$ .

Applying the properties of RBF NN, we have

$$\begin{aligned} -\kappa_i \tilde{W}_i^\top \hat{W}_i &\leq \frac{\kappa_i}{2} \left( \|W_i^*\|^2 - \|\tilde{W}_i\|^2 \right) \\ \|\Theta_i(\hat{Z})\| &\leq \xi_i, \quad \epsilon_i \leq \epsilon_i^* \quad i = 1, 2, 3 \end{aligned} \quad (43)$$

where  $\xi_i, \epsilon_i^*$  are positive constants,  $\varrho_i \leq \rho_{i,0}$ ,  $\dot{\varrho}_i \leq \bar{\varrho}_i$ .

Moreover, using the results of [10, Lemma 3] and [10, Lemma 4], we can conclude that there exist positive constants  $\varsigma_i, i = 1, 2, 3$  satisfying

$$\begin{aligned} \hat{W}_i^\top \Theta_i(\hat{Z}) - W_i^{*\top} \Theta_i(Z) &= W_i^{*\top} (\Theta_i(Z) - \Theta_i(\hat{Z})) \\ &\quad + \tilde{W}_i^\top \Theta_i(\hat{Z}) \\ &\leq \tilde{W}_i^\top \Theta_i(\hat{Z}) + \|W_i^*\| \varsigma_i \end{aligned} \quad (44)$$

Using the Young's inequality, (42) can be rewritten as

$$\begin{aligned} \dot{V} &\leq -(2l_1 - 5/2 - \bar{\varrho}_1/2) e_x^2 - (2l_1 - 5/2 - \bar{\varrho}_2/2) e_y^2 \\ &\quad - (2l_2 - 3/2 - \bar{\varrho}_3/2) e_\psi^2 - (l_3 - 3 - p_1) s_1^2 \\ &\quad - (l_3 - 3 - p_2) s_2^2 - (l_3 - 2 - p_3) s_3^2 \\ &\quad - \sum_{i=1}^3 \frac{\kappa_i}{2} \|\tilde{W}_i\|^2 + C \leq -\mu V + C \end{aligned} \quad (45)$$

where

$$\begin{aligned} \mu &= \min \left( \frac{2l_1 - 5/2 - \bar{\varrho}_1/2}{\rho_{1,0}}, \frac{2l_1 - 5/2 - \bar{\varrho}_2/2}{\rho_{2,0}}, \right. \\ &\quad \left. \frac{2l_2 - 3/2 - \bar{\varrho}_3/2}{\rho_{3,0}}, l_3 - 3 - p_1, \right. \end{aligned}$$

$$l_3 - 3 - p_2, l_3 - 2 - p_3, \min \left( \frac{\kappa_i}{\lambda_{\max}(\Gamma_i^{-1})} \right))$$

$$C = \frac{1}{2} \sum_{i=1}^3 \left( (\kappa_i + \varsigma_i^2/2) \|W_i^*\|^2 + \epsilon_i^{*2} + \bar{\varphi}_i^2 \right)$$

where  $\lambda_{\max}(\bullet)$  denotes the maximum eigenvalues of  $\bullet$ . To guarantee the positive of  $\mu$ , the control gain  $l_1, l_2$  and  $l_3$  should be chosen to satisfy the following conditions:

$$\begin{aligned} l_1 &\geq \max(\bar{\rho}_1/4 + 5/4, \bar{\rho}_2/4 + 5/4), l_2 \geq \bar{\rho}_3/4 + 3/4 \\ l_3 &\geq \max(3 + p_1, 3 + p_2, 2 + p_3) \end{aligned} \quad (46)$$

Multiplying on both sides by  $e^{\mu t}$ , we have

$$V(t) \leq (V(0) - C/\mu) \exp(-\mu t) + C/\mu, \quad \forall t > 0 \quad (47)$$

From the above inequality, and applying the definition of  $V$  in (27), we can draw a conclusion that the transformed errors  $e_x, e_y, e_\psi, s_i$  as well as the NN weight estimation errors  $\tilde{W}_i$  are bounded. In terms of the boundedness of transformed errors and according to Lemma 1, we can conclude that tracking error constraints  $x_e, y_e, \psi_e$  are never violated, i.e.,  $|x_e(t)| < \rho_1(t)$ ,  $|y_e(t)| < \rho_2(t)$ ,  $|\psi_e(t)| < \rho_3(t)$ . This completes the proof.  $\blacksquare$

*Remark 7:* The guidance on how to choose the control parameters are shown as follows.

- 1)  $l_1$  and  $l_2$  in the proposed control relate to the convergent rates of transformed positional errors  $e_x, e_y$  and angular error  $e_\psi$ , respectively. Also,  $l_3$  is associated with the convergent rates of velocity errors  $s_1, s_2$  and  $s_3$ . These parameters should be chosen as positive constants and satisfy the equations (36) and (47) to guarantee stability of the proposed algorithm.
- 2)  $\rho_{i,0}, \rho_{i,\infty}$  and  $\bar{\alpha}_i$  are parameters in the predefined bounded function. To avoid the sharp vibration in the beginning of tracking process,  $\rho_{i,0}$  should be chosen enough large, and  $\bar{\alpha}_i$  should be selected as small as possible. Also,  $\rho_{i,\infty}$  can be suitable chosen according to the accuracy of sensors and actuators that equipped in the USV.
- 3)  $\alpha_1$  and  $\alpha_3$  can influence the compensated rates of saturated inputs, and  $\alpha_2$  will effect the rate to deal with underactuated problem. Moreover,  $\gamma$  is an important parameter for the high gain observer. If  $\gamma$  is selected very large, it will lead to a large estimation error at the beginning of control process.

#### IV. SIMULATIONS

To verify the effectiveness of the proposed controller, we use the USV model from Northwestern Polytechnical University, and these nominal parameters were identified by Unscented Kalman Filter (UKF) via experimental data. The high-gain observer, which is presented in (38) and (39), is designed to estimate the unmeasurable velocities. Logarithmic transformed errors are constructed in (11) to ensure the transient and steady tracking behavior. Furthermore, an adaptive compensating approach in (17) and an state transformation in (13) are designed to address the problems of input saturation, dynamic nonholonomic and dynamic coupled that existing in the realistic situation, respectively.

The nominal parameters are given as follows: (1)  $m_{11}^* = 141.85, m_{22}^* = 191.75, m_{23}^* = 5.7, m_{33}^* = 15.6, m_{12}^* = m_{21}^* = m_{13}^* = m_{31}^* = 0$ ; (2)  $c_{13}^*(v, r) = -191.75v -$

$5.7r, c_{23}^*(u) = 141.85u, c_{31}^*(vr) = 191.75v + 5.7r, c_{32}^*(u) = -141.85u, c_{11}^* = c_{12}^* = c_{21}^* = c_{22}^* = c_{33}^* = 0$ ; (3)  $d_{11}^*(u) = 45.6 + 67.26|u| + 10u^2, d_{22}^*(v, r) = 29.54 + 73.85|v| + 15|r|, d_{23}^*(v, r) = -2.5 + 2|v| + 10.71|r|, d_{32}^*(v, r) = -2.4 - 13|v| - 0.2|r|, d_{33}^*(v, r) = 5.59 + 10.71|r| - 0.07|r|, d_{12}^* = d_{21}^* = d_{13}^* = d_{31}^* = 0$ . Furthermore, the model uncertainty can be assumed as  $\Delta(\eta, \nu) = [0.5, 0.1u^2, 0.1r^2 + \sin(v)]^\top$ .

The desired trajectory is defined as follows: (1)  $0 \leq t < 100$  :  $u_d = 0.5, v_d = 0, r_d = 0$ ; (2)  $100 \leq t < 300$  :  $u_d = 0.5, v_d = 0, r_d = -0.005 \sin(\pi(t - 100)/400)$ ; (3)  $300 \leq t \leq 700$  :  $u_d = 0.5, v_d = 0, r_d = -0.01/2$ . The initial condition of the reference trajectory and the USV are  $\eta_d(0) = [0\text{m}, 0\text{m}, \pi/4 \text{ rad}]^\top$ ,  $\eta(0) = [4\text{m}, -6\text{m}, 0\text{rad}]^\top$ , respectively. The predefined bounded functions are set as  $\rho_1(t) = (20 - 2)e^{-0.05t} + 2$ ,  $\rho_2(t) = (20 - 2)e^{-0.05t} + 2$ ,  $\rho_3(t) = (3 - \pi/9)e^{-0.05t} + \pi/9$ .

To simulate the real oceanic environment, we define the time-varying disturbances in earth frame as

$$w(t) = \begin{bmatrix} -8 + 1.8 \sin(0.7t) + 1.2 \sin(0.05t) + 1.2 \sin(0.9t) \\ -4 + 0.4 \sin(0.1t) + 0.2 \cos(0.6t) \\ 0 \end{bmatrix} \quad (48)$$

Then, the disturbances  $d$  acting on USV in body frame can be expressed as  $d(t) = J^\top(\psi)w(t)$ .

We use RBFNN to approximate the unknown disturbance and uncertain dynamics. 512 NN nodes are used for each  $\Theta_i$ , and the initial weights  $W_i$  are zero. The gain matrices are defined as  $\Gamma_i = 15I_{9 \times 9}$  and the variances are chosen as  $\sigma_i = 8$ , where  $i = 1, 2, 3$ . The input vectors of full back and output feedback controllers are designed as  $Z = [u, \bar{v}, r, u_v, v_v, r_v, e_x, e_y, e_\psi]^\top$  and  $\hat{Z} = [\hat{u}, \hat{v}, \hat{r}, \hat{u}_v, \hat{v}_v, \hat{r}_v, e_x, e_y, e_\psi]^\top$ , respectively. The centres of the neural networks nodes are evenly spaced between the upper and lower bound of the motion range and speed limits of each joint, namely  $\xi_i$  are evenly spaced on  $[0, 0.75] \times [-0.2, 0.2] \times [-0.04, 0.04] \times [0, 0.75] \times [-0.2, 0.2] \times [-0.04, 0.04] \times [-1, 1] \times [-1, 1] \times [-1, 1]$ . Moreover, to compare the control performance, a PI controller is designed as

$$\begin{aligned} \tau_u &= K_{pu} \sqrt{x_e^2 + y_e^2} + K_{iu} \int \sqrt{x_e^2 + y_e^2} dt \\ \tau_r &= K_{pr} \psi_e + K_{ir} \int \psi_e dt \end{aligned} \quad (49)$$

where  $K_{pu} = 12, K_{iu} = 0.005, K_{pr} = -40, K_{ir} = 0$ .

The gains of the adaptive NN control with full state feedback are selected as  $l_1 = 1, l_2 = 2, l_3 = 1, \alpha_1 = 30, \alpha_2 = 50, \alpha_3 = 20, \mu_u = 5, \mu_r = 5, \beta_1(0) = 0, \beta_2(0) = 0, \beta_3(0) = 0, \kappa_1 = 3, \kappa_2 = 1, \kappa_3 = 6$ . Furthermore, the parameters of the adaptive NN control with output feedback are chosen as  $l_1 = 1, l_2 = 2, l_3 = 1, \alpha_1 = 30, \alpha_2 = 50, \alpha_3 = 20, \mu_u = 5, \mu_r = 5, \beta_1(0) = 0, \beta_2(0) = 0, \beta_3(0) = 0, \kappa_1 = 3, \kappa_2 = 6, \kappa_3 = 12$ . Moreover, the parameters of high-gain observer are given as  $\gamma = 0.3, \lambda_1 = 2$ , and the initial terms  $b_1 = [0, 0, 0]^\top, b_2 = [0, 0, 0]^\top$ . The proposed full-state and output feedback control processes are defined as case 1 and case 2, respectively.

Fig. 3 (a) shows that the desired trajectory can be tracked under the proposed adaptive NN controller with full-state and



output feedback. From Figs. 3 (b-d), the tracking errors of the proposed controllers never violate the prescribed constraints, and the errors of the traditional PI controller can violate the prescribed bounds. Moreover, tracking errors of the proposed controllers will converge to a small value close to zero. Figs. 4 (a-b) give the control input  $\tau_u$  and  $\tau_r$ . The norms of NN weights of two NN controllers, which are bounded with slight oscillations, are observed in Fig. 4 (c-d). Fig. 5 shows the observer errors, which indicate the proposed observer can estimate unmeasured velocities.

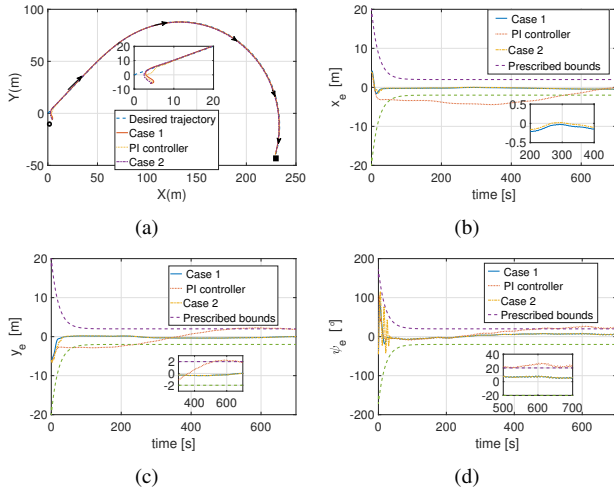


Fig. 3. (a) Trajectory in the horizontal plane. (b) Trajectory tracking error in X. (c) Trajectory tracking error in Y. (d) Trajectory tracking error in  $\psi$ .

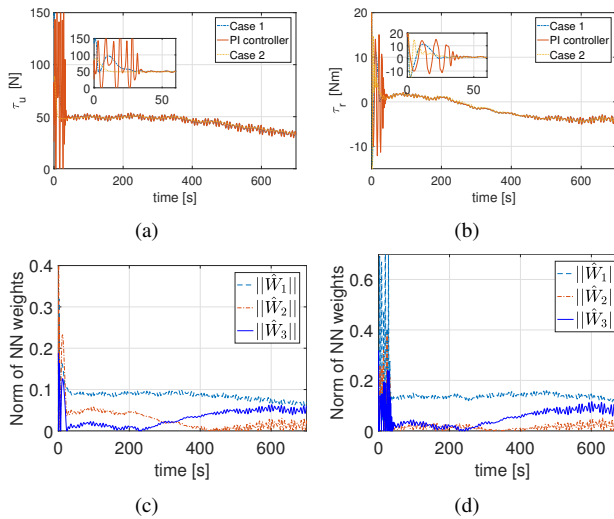


Fig. 4. (a) Control input  $\tau_u$ . (b) Control input  $\tau_r$ . (c) Norm of neural weights for case 1. (d) Norm of neural weights for case 2.

## V. EXPERIMENTS

In this section, we provide experimental results on an USV whose motion is controlled by two propellers. The experimental system, as shown in Fig. 6, owns sensors including IMU and GPS, which are equipped to measure the attitude angle and position, respectively. To carry out the control, the USV runs a C++ program on a 1.8 GHz Industrial Personal Computer

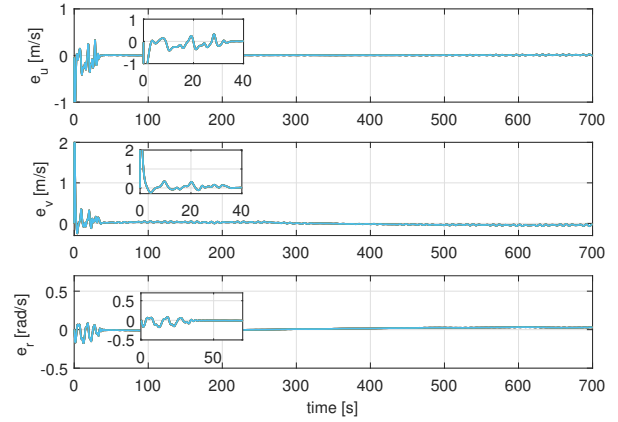


Fig. 5. Observer errors of  $u, v, r$ .

(IPC) platform. The sensor, including IMU and GPS, updates its value every 0.01s, and the control implements every 0.1s. Furthermore, the supervisory computer system is designed to send the sailing mission and to surveillance the sailing states of the USV.

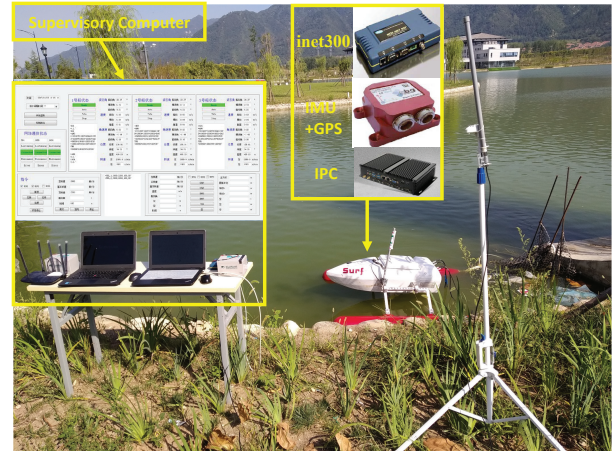


Fig. 6. Illustration of the setup of the experiment.

The nominal parameters are identified by UKF via experimental data. The desired trajectory is initialized at  $\eta_d(0) = [5\text{m}, 0\text{m}, 0\text{rad}]^T$ . The desired trajectory is defined as follows:  $0 \leq t \leq 90$ :  $u_d = \pi/5, v_d = 0, r_d = \pi/100$ . The bounded functions, hydrodynamic coefficients and input limits are defined the same as the ones in simulation part.

The gains of the experimental output feedback controller are selected as  $l_1 = 1.8, l_2 = 2.4, l_3 = 1.9, \alpha_1 = 10, \alpha_2 = 30, \alpha_3 = 20, \mu_u = 5, \mu_r = 5, \beta_1(0) = 0, \beta_2(0) = 0, \beta_3(0) = 0, \kappa_1 = 2.3, \kappa_2 = 4.5, \kappa_3 = 6$ . Moreover, the parameters of high-gain observer are given as  $\gamma = 0.1, \lambda_1 = 1.2$ , and the initial terms  $b_1 = [0, 0, 0]^T, b_2 = [0, 0, 0]^T$ . The parameters of PI controller are chosen as  $K_{pu} = 16.2, K_{iu} = 0.002, K_{pr} = -30, K_{ir} = 0$ .

The main purpose of the experiment is to validate the proposed output feedback controller. The diagram of the USV control system is illustrated in Fig. 2. Fig. 8 (a) shows that the desired trajectory can be tracked under the adaptive NN

controller with output state feedback. Fig. 8 (b) gives the estimated values of NNs. Fig. 7 gives the control input of two propellers. Figs. 8(c)-(e) describe that the tracking errors of the proposed controller never violate the prescribed constraints. Figs. 8(f)-(h) give the estimated values of state  $u, v, r$ .

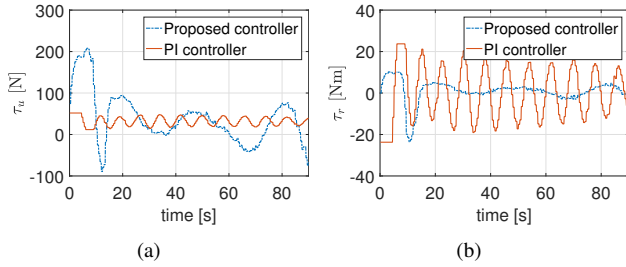


Fig. 7. Control input (a)  $\tau_u$ . (b)  $\tau_r$ .

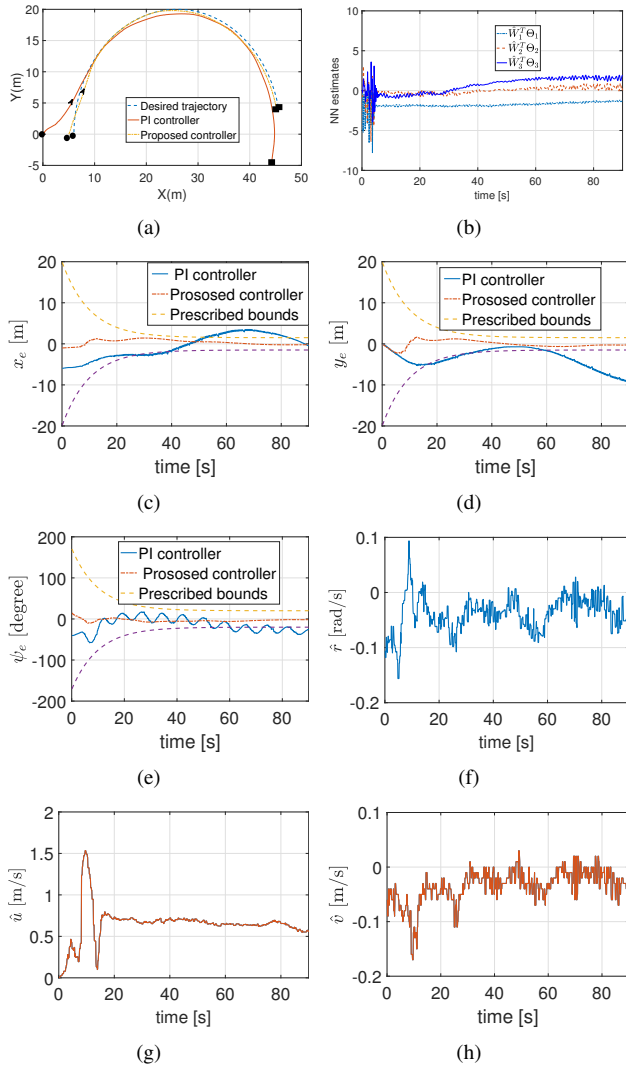


Fig. 8. Experimental results (a)Trajectory in X-Y plane, (b)estimated values of NN, (c)  $x_e$ , (d)  $y_e$ , (e)  $\psi_e$ , (f) $\hat{r}$ , (g) $\hat{u}$ , (h) $\hat{v}$ .

## VI. CONCLUSION

In this paper, an adaptive trajectory tracking controller with guaranteed transient performance is developed for a general

type of the USV. The NNs are used to approximate the unknown external disturbances and model uncertainties. To reflect more realistic situation, we simultaneously consider the input saturation problem and realistic dynamical model of the USV that the mass and damping matrices are not diagonal. Furthermore, simulation and experimental results show the superior performance of the proposed controller.

## REFERENCES

- [1] Z. Zhang, Y. Shi, Z. Zhang, and W. Yan, "New results on sliding-mode control for takagisugeno fuzzy multiagent systems," *IEEE Transactions on Cybernetics*, vol. 49, no. 5, pp. 1592–1604, 2019.
- [2] R. Yu, Q. Zhu, G. Xia, and Z. Liu, "Sliding mode tracking control of an underactuated surface vessel," *Control Theory & Applications*, vol. 6, no. 3, pp. 461–466, 2012.
- [3] H. Ashrafiuon, K. R. Muske, L. C. McNinch, and R. A. Soltan, "Sliding-mode tracking control of surface vessels," *IEEE Transactions on Industrial Electronics*, vol. 55, no. 11, pp. 4004–4012, 2008.
- [4] M. Chen, S. S. Ge, B. V. E. How, and Y. S. Choo, "Robust adaptive position mooring control for marine vessels," *IEEE Transactions on Control Systems Technology*, vol. 21, no. 2, pp. 395–409, 2013.
- [5] L. Qiu, Y. Shi, J. Pan, B. Zhang, and G. Xu, "Collaborative tracking control of dual linear switched reluctance machines over communication network with time delays," *IEEE Transactions on Cybernetics*, vol. 47, no. 12, pp. 4432–4442, 2017.
- [6] B. S. Park, J. W. Kwon, and H. Kim, "Neural network-based output feedback control for reference tracking of underactuated surface vessels," *Automatica*, vol. 77, pp. 353–359, 2017.
- [7] Z. Peng, J. Wang, and Q. L. Han, "Path-following control of autonomous underwater vehicles subject to velocity and input constraints via neurodynamic optimization," *IEEE Transactions on Industrial Electronics*, 2019, doi:10.1109/TIE.2018.2885726.
- [8] Z. Peng, J. Wang, and J. Wang, "Constrained control of autonomous underwater vehicles based on command optimization and disturbance estimation," *IEEE Transactions on Industrial Electronics*, vol. 66, no. 5, p. 3627–3635, 2019.
- [9] S. He, S. L. Dai, and F. Luo, "Asymptotic trajectory tracking control with guaranteed transient behavior for msv with uncertain dynamics and external disturbances," *IEEE Transactions on Industrial Electronics*, vol. 66, no. 5, pp. 3712–3720, 2019.
- [10] W. He, Z. Yin, and C. Sun, "Adaptive neural network control of a marine vessel with constraints using the asymmetric barrier lyapunov function," *IEEE transactions on cybernetics*, vol. 47, no. 7, pp. 1641–1651, 2017.
- [11] X. Xiang, C. Yu, and Q. Zhang, "On intelligent risk analysis and critical decision of underwater robotic vehicle," *Ocean Engineering*, vol. 140, pp. 453–465, 2017.
- [12] Z. Peng, D. Wang, Z. Chen, X. Hu, and W. Lan, "Adaptive dynamic surface control for formations of autonomous surface vehicles with uncertain dynamics," *IEEE Transactions on Control Systems Technology*, vol. 21, no. 2, pp. 513–520, 2013.
- [13] L. Ding, S. Li, Y.-J. Liu, H. Gao, C. Chen, and Z. Deng, "Adaptive neural network-based tracking control for full-state constrained wheeled mobile robotic system," *IEEE Transactions on Systems, Man, and Cybernetics: Systems*, vol. 47, no. 8, pp. 2410–2419, 2017.
- [14] S. L. Dai, M. Wang, C. Wang, and L. Li, "Learning from adaptive neural network output feedback control of uncertain ocean surface ship dynamics," *International Journal of Adaptive Control & Signal Processing*, vol. 28, no. 15, pp. 341–365, 2014.
- [15] S. L. Dai, M. Wang, and C. Wang, "Neural learning control of marine surface vessels with guaranteed transient tracking performance," *IEEE Transactions on Industrial Electronics*, vol. 63, no. 3, pp. 1717–1727, 2016.
- [16] C. Yang, K. Huang, H. Cheng, Y. Li, and C. Y. Su, "Haptic identification by elm-controlled uncertain manipulator," *IEEE Transactions on Systems Man & Cybernetics Systems*, vol. 47, no. 8, pp. 2398–2409, 2017.
- [17] C. Shen, Y. Shi, and B. Buckham, "Path-following control of an auv: A multi-objective model predictive control approach," *IEEE Transactions on Control Systems Technology*, vol. 27, no. 3, pp. 1334–1342, 2019.
- [18] —, "Trajectory tracking control of an autonomous underwater vehicle using lyapunov-based model predictive control," *IEEE Transactions on Industrial Electronics*, vol. 65, no. 7, pp. 5796–5805, 2018.
- [19] H. Hjalmarsson, M. Gevers, S. Gunnarsson, and O. Lequin, "Iterative feedback tuning: Theory and applications," *IEEE Control Systems Magazine*, vol. 38, no. 4, pp. 26–41, 1998.

[20] M.-B. Radac, R.-E. Precup, E. M. Petriu, and S. Preitl, "Iterative data-driven tuning of controllers for nonlinear systems with constraints," *IEEE Transactions on Industrial Electronics*, vol. 61, no. 11, pp. 6360–6368, 2014.

[21] Z. Wang, R. Lu, F. Gao, and D. Liu, "An indirect data driven method for trajectory tracking control of a class of nonlinear discrete-time systems," *IEEE Transactions on Industrial Electronics*, vol. 64, no. 5, pp. 4121–4129, 2017.

[22] C. Hu, R. Wang, F. Yan, and N. Chen, "Robust composite nonlinear feedback path following control for underactuated surface vessels with desired-heading amendment," *IEEE Transactions on Industrial Electronics*, vol. 63, no. 10, pp. 6386–6394, 2016.

[23] X. Lei, S. S. Ge, and J. Fang, "Adaptive neural network control of small unmanned aerial rotorcraft," *Journal of Intelligent & Robotic Systems*, vol. 75, no. 2, pp. 331–341, 2014.

[24] S. Blai, I. Skrjanc, and D. Matko, "Globally stable direct fuzzy model reference adaptive control," *Fuzzy Sets & Systems*, vol. 139, no. 1, pp. 3–33, 2003.

[25] J. Ghommam, F. Mnif, A. Benali, and N. Derbel, "Asymptotic backstepping stabilization of an underactuated surface vessel," *IEEE Transactions on Control Systems Technology*, vol. 14, no. 6, pp. 1150–1157, 2006.

[26] C. P. Bechlioulis and G. A. Rovithakis, "Brief paper: Adaptive control with guaranteed transient and steady state tracking error bounds for strict feedback systems," *Automatica*, vol. 45, no. 2, pp. 532–538, 2009.

[27] C. P. Bechlioulis, G. C. Karras, S. Heshmati-Alamdari, and K. J. Kyriakopoulos, "Trajectory tracking with prescribed performance for underactuated underwater vehicles under model uncertainties and external disturbances," *IEEE Transactions on Control Systems Technology*, vol. 25, no. 2, pp. 429–440, 2016.

[28] O. Elhaki and K. Shojaei, "Neural network-based target tracking control of underactuated autonomous underwater vehicles with a prescribed performance," *Ocean Engineering*, vol. 167, pp. 239–256, 2018.

[29] Z. Zheng and M. Feroskhan, "Path following of a surface vessel with prescribed performance in the presence of input saturation and external disturbances," *IEEE/ASME Transactions on Mechatronics*, vol. 22, no. 6, pp. 2564–2575, 2017.

[30] K. D. Do and J. Pan, "Global tracking control of underactuated ships with nonzero off-diagonal terms in their system matrices," *Automatica*, vol. 41, no. 1, pp. 87–95, 2005.

[31] S. J. Yoo and B. S. Park, "Guaranteed performance design for distributed bounded containment control of networked uncertain underactuated surface vessels," *Journal of the Franklin Institute*, vol. 354, no. 3, pp. 1584–1602, 2017.

[32] L. P. Perera and C. G. Soares, "Pre-filtered sliding mode control for nonlinear ship steering associated with disturbances," *Ocean Engineering*, vol. 51, no. 3, pp. 49–62, 2012.

[33] L. J. Zhang, H. M. Jia, and X. Qi, "Nnffc-adaptive output feedback

trajectory tracking control for a surface ship at high speed," *Ocean Engineering*, vol. 38, no. 13, pp. 1430–1438, 2011.

[34] S. Roy, S. B. Roy, and I. N. Kar, "Adaptive robust control of euler-lagrange systems with linearly parametrizable uncertainty bound," *IEEE Transactions on Control Systems Technology*, vol. 26, no. 5, pp. 1842–1850, 2018.

[35] C. Wen, J. Zhou, Z. Liu, and H. Su, "Robust adaptive control of uncertain nonlinear systems in the presence of input saturation and external disturbance," *IEEE Transactions on Automatic Control*, vol. 56, no. 7, pp. 1672–1678, 2011.



**Rongxin Cui** (M'09) received the B.Eng. degree in automatic control and the Ph.D. degree in control science and engineering from Northwestern Polytechnical University, Xian, China, in 2003 and 2008, respectively.

From August 2008 to August 2010, he worked as a Research Fellow at the Centre for Offshore Research & Engineering, National University of Singapore, Singapore. Currently, he is a Professor with the School of Marine Science and Technology, Northwestern Polytechnical University, Xi'an, China. His current research interests are control of nonlinear systems, cooperative path planning and control for multiple robots, control and navigation for underwater vehicles, and system development.

Dr. Cui serves as an Editor for the *Journal of Intelligent and Robotic Systems* and an Associate Editor for the IEEE TRANSACTIONS ON SYSTEMS, MAN, AND CYBERNETICS: SYSTEMS.



**Chenguang Yang** (M'10-SM'16) is a Professor of Robotics. He received the Ph.D. degree in control engineering from the National University of Singapore, Singapore, in 2010 and performed postdoctoral research in human robotics at Imperial College London, London, UK from 2009 to 2010. He has been awarded EU Marie Curie International Incoming Fellowship, UK EPSRC UKRI Innovation Fellowship, and the Best Paper Award of the IEEE Transactions on Robotics as well as over ten conference Best Paper Awards.

His research interest lies in human robot interaction and intelligent system design.



**Lepeng Chen** received B.Eng. degree in automatic control from Northwestern Polytechnical University, Xi'an, China, in 2015.

He is currently pursuing the Ph.D. degree at the School of Marine Science and Technology, Northwestern Polytechnical University, Xi'an, China. His research interests are adaptive control and its applications to marine vehicles.



**Weisheng Yan** received the B.Eng. degree in automatic control and the Ph.D. degree in navigation, guidance, and control from Northwestern Polytechnical University, Xian, China, in 1991 and 1999, respectively. He is currently a Professor with the School of Marine Science and Technology, Northwestern Polytechnical University. His current research interests include guidance, navigation, and control of underwater vehicles.